*Korean J. Chem. Eng.*, **20**(1), 110-115 (2003)

# Hydrodynamic Characteristics of a FCC Regenerator

**Won Namkung*, Sung Won Kim and Sang Done Kim†**

Department of Chemical and Biomolecular Engineering and Energy & Environment Research Center, Korea Advanced Institute of Science and Technology, Daejeon 305-701, Korea
(*Received 26 February 2002 • accepted 30 May 2002*)

**Abstract**−The hydrodynamic and gas mixing characteristics have been determined in a FCC regenerator (0.48 m I.D.×3.4 m high) with FCC particles. Solids holdup in the dense bed decreases with increasing gas velocity, but it increases in the freeboard region. The bubble/void fraction increases with an increase along the bed height at a given gas velocity and increases with increasing gas velocity at a constant bed height. Backmixed tracer gas at the wall region is higher than that at the center region of the bed. The gas backmixing coefficient decreases with increasing gas velocity.

Key words: FCC Regenerator, Bubble/Void, Gas Mixing

## INTRODUCTION

The Fluid Catalytic Cracking (FCC) unit has been used to convert heavy oil to gasoline. To date, about 350 FCC plants have been operating and new FCC plants are being built annually [Senior and Avidan, 1996].

In a FCC unit, FCC catalysts are circulated rapidly between riser and regenerator where the catalyst is regenerated. A FCC regenerator is used to burn coke-deposited catalyst for restoring catalyst activity and supply heat to the riser for the cracking reaction. It is known that bubble or void properties such as bubble/void velocity and fraction have a strong influence on both heat and mass transfers in fluidized beds [Farag et al., 1997]. Also, for practical design purposes an understanding of gas mixing characteristics is needed to evaluate gas flow patterns in a fluidized bed. To date many studies have been carried out in the risers where gas-solid reactions occur. However, studies on solids and gas flow behaviors in the regenerator are comparatively sparse though it affects total performance of FCC unit [Kim et al., 2000].

In the present study, bubble/void and gas mixing characteristics in the FCC regenerator have been determined.

## EXPERIMENTAL

Experiments were performed in the upper and lower parts of a FCC regenerator made of a transparent Plexiglas column as shown in Fig. 1(a). The diameters of the upper and lower part regenerators were 0.48 m and 0.26 m, respectively. The upper parts of each regenerator were expanded to 0.90 m (upper) and 0.48 m (lower) to reduce particle entrainment, respectively. The gas distributors of the upper and lower regenerators are shown in Fig. 1(b). The solid feeder, including a hopper in the upper part regenerator, and a stor-

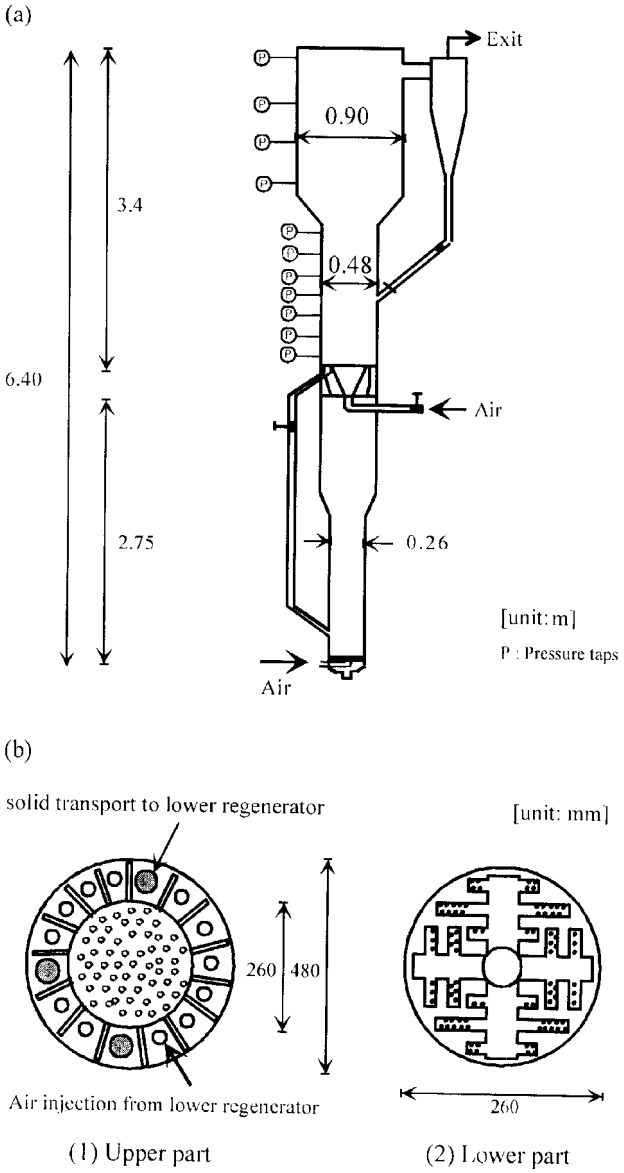


**Fig. 1. Schematic diagram of FCC regenerator: (a) experimental apparatus, (b) distributors of regenerators.**

†To whom correspondence should be addressed.
E-mail: kimsd@kaist.ac.kr
*Present address: Smelting Reduction Research Team, RIST, Pohang 790-600, Korea
‡This paper is dedicated to Professor Dong Sup Doh on the occasion of his retirement from Korea University.

age tank at the exit of the lower part regenerator were installed to provide continuous solids feeding from the upper to the lower regenerators. Air was injected into the two regenerators, and injected air at the lower part of the regenerator was re-injected into the upper regenerator through pipes around the distributor. Pressure taps were mounted flush with the wall of the column and connected to a manometer or pressure transducer to measure pressure drops from which the cross-sectional averaged voidage in the regenerators was deduced. The pressure signals from the pressure transducer were amplified and sent via an A/D converter to a personal computer for recording. The differential pressure fluctuation was measured with a pressure transducer (Valydine P306D, USA). The mean diameter and apparent density of spent FCC particles used as the bed materials were 70 μm and 2,130 kg/m$^3$, respectively. In this study, gas velocity ($U_g$) in the upper regenerator was varied from 0.56 to 1.15 m/s, and that in the lower regenerator was fixed at 1.00 m/s, as in a commercial reactor. The gas velocity ($U_g$) in the upper regenerator is velocity considering air re-injected from the lower regenerator.

A transmission type optical fiber probe was used to determine the bubble/void properties. The details of the probe system can be found elsewhere [Lee and Kim, 1991]. A schematic diagram and typical output signal from the optical fiber probe system are shown in Fig. 2. The optical fiber probe consisted of two pairs of optical fibers with a diameter of 500 μm. One pair was a light projector from the light source of a Helium-Neon laser (17 mW, Uniphase Model 1144, USA), and the other opposite side was a receiver of the light transmitted that was connected to a phototransistor, amplifier, A/D converter and a personal computer. The sampling interval of signals was selected at 500 μs and the data were collected during the sampling time of 30 s for each experimental condition.

The tracer gas (He) was injected to determine gas mixing at steady state as step injection at 0.4 m above the distributor plate through an up-facing injection hole. The tracer injection rate was 0.45-0.56% by volume of the total air flow rate. The holes of the sampling tube were covered with a screen to prevent leakage of solid particles from the bed. The tracer gas was sampled at 0.1, 0.2 m below and 0.8 m above the injection point. To determine the gas backmixing coefficient, the injection and sampling tubes were moved radially across the bed width. At steady state conditions, the tracer gas was sampled at nine different radial positions and the sampled gas was analyzed by gas chromatography (HP 5890II, USA).

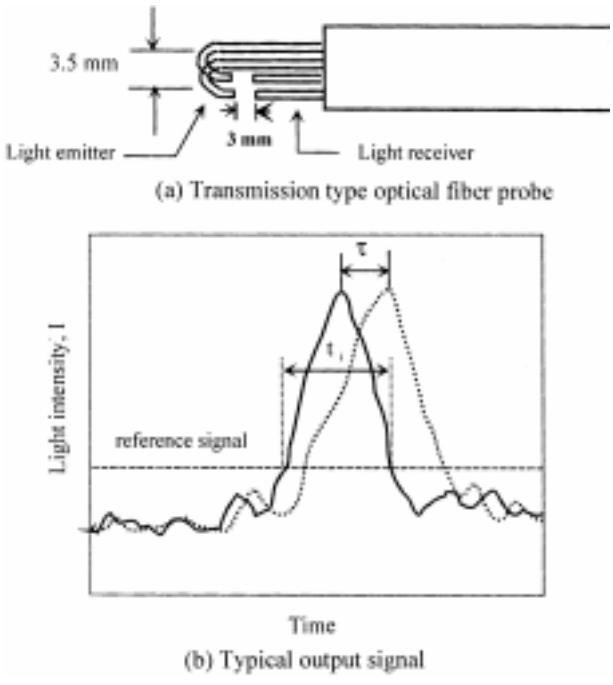


**Fig. 2. Optical fiber probe and typical output signal.**

## RESULTS AND DISCUSSION

### 1. Axial Solids Holdup

The effect of gas velocity on axial solids holdup distribution in the upper regenerator is shown in Fig. 3. The initial bed height was 0.50 m and gas velocity was varied from 0.56 to 1.15 m/s. As shown in Fig. 3, the axial solids holdup distribution exhibits a typical solids holdup distribution in a turbulent bed with dense region in the bottom of the reactor and dilute region in the freeboard region. The gradient of axial solids holdup distribution decreases with increasing gas velocity. As the gas velocity is increased, solids holdup in the bottom region decreases, but it increases in the freeboard region due to the increase of particle entrainment from dense region to freeboard region. Solids holdup decreases exponentially with height above the dense bed. The solids downflow near the wall region in the freeboard was observed with increasing $U_g$ due to formation of the core-annulus structure at higher $U_g$ [Namkung and Kim, 1998a]. Therefore, the regenerator has the flow structure of gas-solid upflow in the core region and solid down-flow near the wall region at the given operating range of $U_g$. The lower regenerator has a similar axial solids holdup distribution as in the upper regenerator. Although solids holdup at 1.5 m above the distributor is not largely

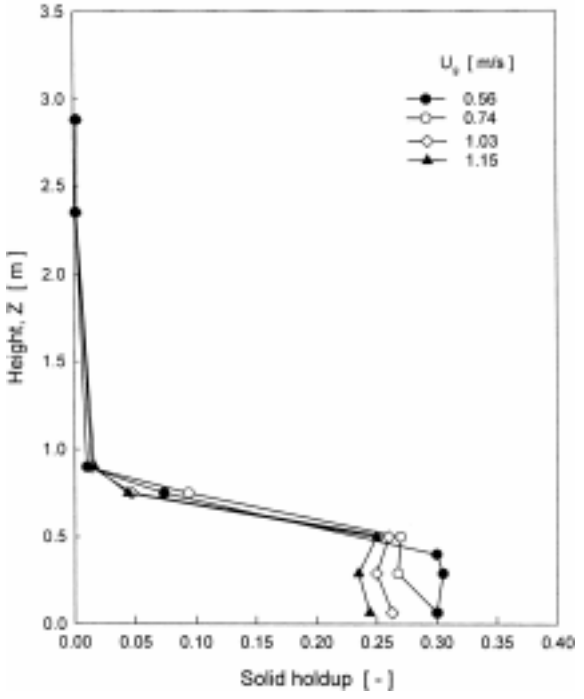


**Fig. 3. Effect of gas velocity on axial solid holdup profile in the upper regenerator.**

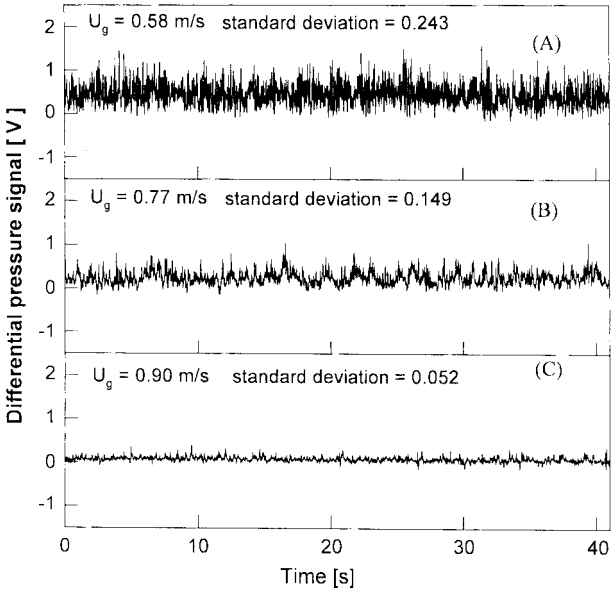


**Fig. 4. Pressure fluctuation from differential transducer.**

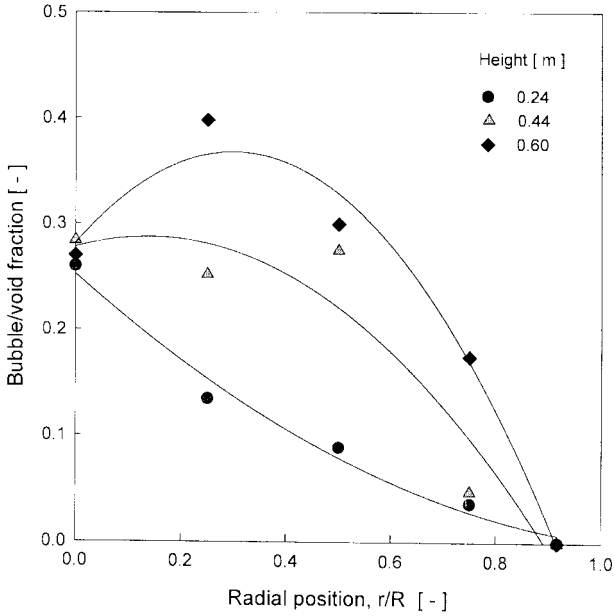


**Fig. 5. Radial profile of bubble/void fraction ($U_g$=1.03 m/s).**

varied with gas velocity due to the expansion of reactor, solids holdup at 1.2 m (freeboard region) from the distributor increases with increasing gas velocity due to the increase of entrainment.

The flow behavior with gas velocity can be predicted indirectly by measuring pressure fluctuation in the bed as shown in Fig. 4 at steady state in the upper part regenerator. Pressure fluctuation was measured at 0.09-0.14 m above the distributor by using a pressure transmitter. The sampling interval of signals was selected at 10 ms, and the signals were collected during a sampling time of 41 s for each experimental condition. Pressure fluctuations are affected by solid and bubble flows in the bed. Standard deviation of pressure drop initially increases with increasing gas velocity, though it goes to a maximum value at a given gas velocity, and then sharply decreases with increasing gas velocity [Namkung et al., 2000]. The gas velocity at which the maximum standard deviation occurs can be regarded as a transition velocity from bubbling to turbulent fluidized bed. The transition velocity of FCC particle in this study is 0.65 m/s [Kim et al., 2000]. Therefore, Fig. 4(A) indicates the pressure fluctuation in the bubbling fluidized bed. Whereas, Figs. 4(B) and (C) are pressure fluctuations in the turbulent fluidized bed. As shown in Fig. 4, standard deviation of pressure fluctuation decreases with increasing $U_g$ in the turbulent fluidized bed. This means that the bed becomes more homogeneous as $U_g$ increases in the turbulent fluidized bed. The mean pressure drop decreases with increasing gas velocity due to the decrease of solids holdup with increasing $U_g$ in the bed.

## 2. Bubble/Void Characteristics

A time series analysis [Bendat and Pieslo, 1986] was performed on the signals from the probe before calculation of the bubble properties. The time lag ($\tau$) between two tips (d) was calculated by the cross-correlation [Farag et al., 1997]. Thus, a local time averaged bubble/void velocity and the average bubble/void rising velocity can be calculated as follows, respectively:

$$U_{bi}=\frac{d}{\tau} \tag{1}$$

$$U_b=\frac{1}{n}\sum_{i=1}^{n}U_{bi} \tag{2}$$

The bubble/void chord length can be calculated from contacting time ($t_i$) of bubble/void with the tip as:

$$L_i=U_b\times t_i \tag{3}$$

The bubble/void fraction was determined as follows:

$$\delta=\frac{\sum_{i=1}^{n}t_i}{T} \tag{4}$$

where T is total sampling time.

The bubble/void fraction with the radial direction (r/R) in the upper regenerator is shown in Fig. 5. The gas velocity in the regenerator was 1.03 m/s and the initial bed height was 0.7 m. Bubble/void velocity is higher at the center region, and it increases with increasing bed height. As can be seen in Fig. 5, the local bubble/void fraction exhibits a spatial non-uniformity. The local bubble/void fraction has higher values in the center region and decreases towards the wall region of the bed, which corresponds to the distribution of bubble chord length in a previous study [Clift and Grace, 1985]. The bubble fraction near the wall region is near to zero as in the bubbling beds due to solid circulation pattern in the bed [Clift and Grace, 1985]. In the bed, bubble flows toward the center of the bed as the bed height increases and solids flow downwards close to the wall region of the bed. The down-flow solids may suppress the bubble activity. Farag et al. [1997] reported that bubble fractions in the centerline of reactor (0.50 m I.D.) are low, whereas high fractions were obtained in this study. This difference may come from the different types of distributors employed. In this study, a large fraction of fresh air was injected through the center region of the distributor (Fig. 1).

The effect of gas velocity on the area-mean bubble fraction is shown in Fig. 6 where the fraction increases with increasing gas ve-

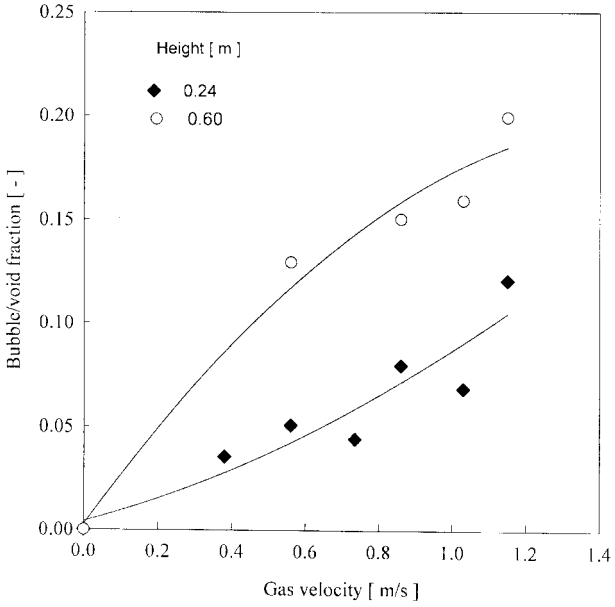


**Fig. 6. Effect of gas velocity on area-mean bubble fraction.**

locity. The bubble/void fraction is governed by its length and frequency [Choi and Kim, 1991; Kim et al., 2000]. The fraction increases due to the increase of frequency and elongation of bubbles with increment of $U_g$ [Kim et al., 1998]. Also, this is deduced indirectly from the results of solid holdup that decreases with increasing $U_g$ in the bed. The bubble/void fraction is higher due to the presence of larger bubbles at the higher bed height (0.6 m) [Choi and Kim, 1991; Farag et al., 1997].

The distributions of bubble/void velocity ($U_b$) and the radial chord length in the bed with solids flow are shown in Fig. 7. The gas velocity in the upper regenerator was 0.93 m/s and solid flow rate was 53.5 kg/h. The distribution of $U_b$ exhibits a similar trend in the bubbling fluidized bed. The bubble flow rate has a local maximum value in the annular ring region near periphery of the bed. This maximum value amplifies and moves inwards with the bed height, eventually reaching the center of the column due to bubble coalescence. The radial bubble chord length also exhibits spatial non-uniformity with a maximum value in the annular ring near the periphery of the bed due to the non-uniform gas supplied to the distributor in the regenerator. Bubble chord length in the center region near the distributor is comparatively larger due to bubble coalescence.

In the bed with solids flow, bubble/void velocity and chord length are not affected largely by solids flow because the injection and exit regions were relatively small compared to the total area as in the commercial FCC regenerator as shown in Fig. 1 [Wilson, 1997]. Therefore, it may be claimed that the present data of bubble/void properties can be used to estimate the bubble/void properties in a regenerator with solids flow.

## 3. Gas Mixing

The radial concentration profiles of the tracer gas (He) that is injected at the center of the bed 0.4 m above the distributor are shown in Fig. 8. As can be seen, the tracer concentration profiles above and below the injection point exhibit different concentration profiles. As shown in Fig. 5, bubble/void fraction at the center region is higher than that at the wall region and gas-solid flows upward. On the other hand, void fraction approaches near to zero due to the downflow of solid near the wall region. The injected tracer gas at the center region flows upward by gas-solid flow, and it transfers to the wall region by mass transfer due to the radial mixing. Then, the transferred tracer gas into the wall region is backmixed due to

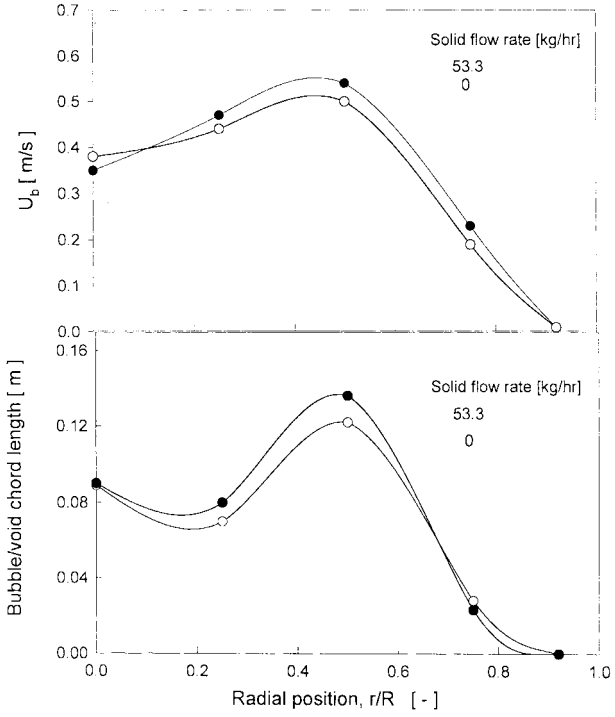


**Fig. 7. Radial profile of bubble/void velocity and bubble/void chord length with and without solids flow.**

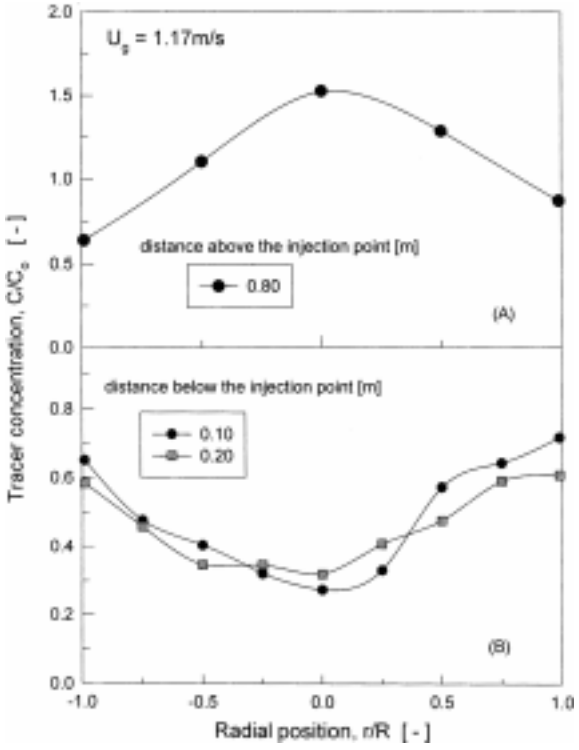


**Fig. 8. Tracer gas concentration profiles at $U_g$=1.17 m/s.**

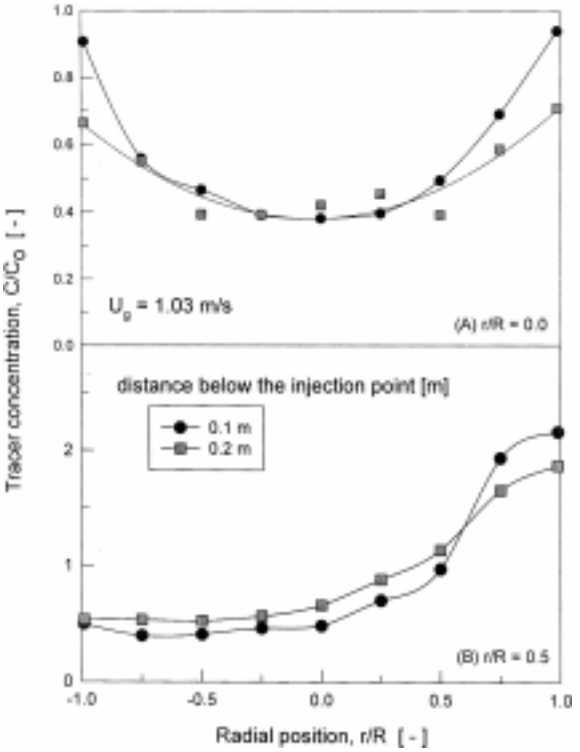


**Fig. 9. Radial concentration profile of backmixed tracer gas at $U_g$= 1.03 m/s.**

the downflow of solids. Therefore, the concentration profile of tracer above the injection point exhibits a maximum value at the center of the bed (Fig. 8A). While, backmixed tracer concentration at the center below the injection point is lower than that near the wall (Fig. 8B) region due to the upward flow of gas-solid phases in the center region.

The radial concentration distribution of backmixed tracer gas at $U_g$=1.03 m/s is shown in Fig. 9. As can be seen, the backmixed tracer concentration is higher when the tracer gas was injected at r/R=0.5 (Fig. 9B) than that of gas injection at r/R=0.0 (Fig. 9A). When the tracer gas was injected at the center region, the backmixed tracer concentration decreased with increasing gas velocity ($U_g$=1.03→1.17 m/s). It indicates that gas backmixing decreases with increasing $U_g$. As can be seen in Fig. 6, bubble/void fraction increases and solids holdup decreases as gas velocity is increased. When the tracer gas was injected at r/R=0.5 (Fig. 9B), a considerable amount of backmixed tracer gas could be detected near the wall below the injection point due to the downflow of solids. In a small column, the tracer concentration of the opposite side of the injection point is slightly higher than that of center region due to the circumferential mixing [Namkung and Kim, 1998a, b]. However, in this study, the increase of tracer gas concentration at the opposite side of the injection point was not observed in a comparatively larger diameter (0.48 m) column.

In general, the gas backmixing coefficients have been determined by using the dispersion model based on one-dimensional flow [Namkung and Kim, 1999].

The axial dispersion model at steady state can be expressed as

$$\varepsilon D_b \frac{d^2C}{dx^2} - \varepsilon \frac{U_g}{\varepsilon}\frac{dC}{dx} = 0 \quad (5)$$

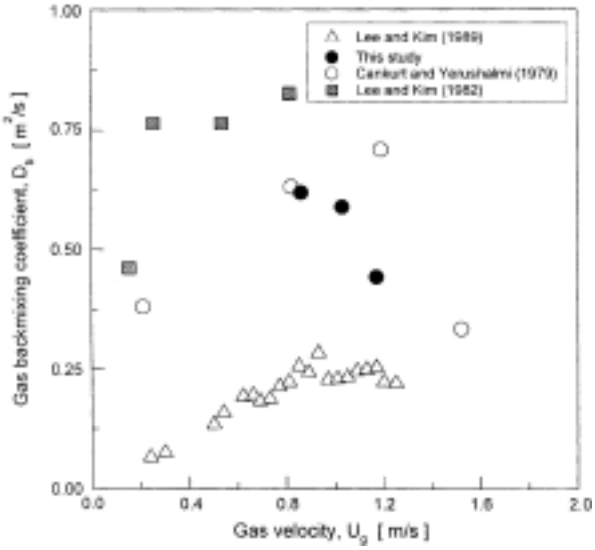


**Fig. 10. Effect of gas velocity on gas backmixing coefficient.**

with the following boundary conditions

$$x=0,\ C/C_o=1,\ x=-\infty,\ C/C_o=0 \quad (6)$$

Then, Eq. (5) has a solution of the form as:

$$\frac{C}{C_o} = \exp\left(\frac{U_g}{\varepsilon D_b}x\right) \quad (7)$$

where $C_o$ and $D_b$ are the mean concentration of tracer gas at the injection level and the gas backmixing coefficient, respectively. The gas backmixing coefficient ($D_b$) can be obtained from the slope of $C/C_o$ vs. x by using the measured solid holdup.

The effect of gas velocity on $D_b$ is shown in Fig. 10. As can be seen, $D_b$ decreases with increasing $U_g$. In the turbulent flow region, it is known that $D_b$ decreases contrary to the bubbling region where $D_b$ increases with increasing $U_g$ [Lee and Kim, 1989: Cankurt and Yerushalmi, 1978]. However, until now, the effect of $U_g$ on $D_b$ in the turbulent region has not been completely understood. Lee and Kim [1989] and Cankurt and Yerushalmi [1978] reported that $D_b$ exhibits a maximum value with variation of $U_g$ in the bubbling and turbulent fluidized beds. In this study, the maximum value of $D_b$ with $U_g$ has not been found because the experiments were performed in the turbulent region.

## CONCLUSIONS

Solids holdup in the dense bed decreases and that in the freeboard region increases with increasing gas velocity in the regenerator. Standard deviation of pressure fluctuation in the bed decreases with increasing gas velocity. The bubble/void fraction increases along the regenerator height with increasing gas velocity. Backmixed tracer gas at the wall region is higher than that at the center region due to the downflow of solids. However, gas backmixing is negligibly small at the center region of the bed. The gas backmixing coefficient decreases with increasing gas velocity. The gas-solid flow pattern in the regenerator at turbulent fluidizing state can be predicted by the bubble/void and gas mixing characteristics. Most of the gas-solid

flows upward at the center region, while solids are downflow near the wall region of the regenerator.

## ACKNOWLEDGMENT

We acknowledge a Grant-in-Aid for research from the SK Corporation, Korea.

## NOMENCLATURE

C : concentration of tracer gas [mol/$m^3$]
$C_o$ : mean concentration of tracer gas at injection level [mol/$m^3$]
$D_b$ : gas backmixing coefficient [$m^2$/s]
d : distance between probe tips [m]
r : radial position [m]
R : regenerator radius [m]
t : contacting time of a void with tip of probe [s]
T : total sampling time [s]
$U_{bi}$ : bubble rising velocity [m/s]
$U_b$ : average bubble rising velocity [m/s]
$U_g$ : gas velocity [m/s]
x : vertical distance from the tracer gas injection [m]

### Greek Letters

$\delta$ : void fraction [-]
$\varepsilon$ : voidage [-]
$\tau$ : time delay determined by cross correlation [s]

## REFERENCES

Bendat, J. S. and Piersol, A. G., "Random Data, Analysis and Measurement Procedures," John Wiley & Sons, New York, 361 (1986).

Cankurt, N. T. and Yerushalmi, J., "Gas Backmixing in High Velocity Fluidized Beds," Fluidization, Davidson, J. F. and Kearins, D. L., eds., Cambridge Univ. Press, London, 387 (1978).

Choi, Y. T. and Kim, S. D., "Bubble Characteristics in an Internally Circulating Fluidized Bed," *J. Chem. Eng. Japan*, **24**, 195 (1991).

Clift, R. and Grace, J. R., "Fluidization," Davidson, J. F., Harrison, D. and Clift, R., eds., Academic Press Inc., London, 73 (1985).

Farag, H. I., Ege, P. E., Grislingas, A. and de Lasa, H. I., "Flow Patterns in a Pilot Plant-Scale Turbulent Fluidized Bed Reactor: Concurrent Application of Tracers and Fiber Optic Sensors," *Can. J. Chem. Eng*., **75**, 851 (1997).

Kim, S. W., Namkung, W. and Kim, S. D., "Bubble/void Properties in a FCC Regenerator," Proc. 6th Asian Conf. on Fluidized-bed and Three-phase Reactors, eds. by H. S. Chun and S. D. Kim, Cheju, Korea, 43 (1998).

Kim, S. W., Namkung, W. and Kim, S. D., "Solids Behavior in Freeboard of FCC Regenerator," *J. Chem. Eng. Japan*, **33**, 78 (2000).

Lee, G. S. and Kim, S. D., "Gas Mixing in Slugging and Turbulent Fluidized Beds," *Chem. Eng. Commun*., **86**, 91 (1989).

Lee, G. S. and Kim. S. D., "Void Characteristics in Turbulent Fluidized Beds," *Korean J. Chem. Eng*., **8**, 6 (1991).

Namkung, W. and Kim, S. D., "Gas Backmixing in a Circulating Fluidized Bed," *Powder Technology*, **99**, 70 (1998a).

Namkung, W. and Kim, S. D., "Gas Mixing Characteristics in a Fast Fluidized Bed," *HWAHAK KONGHAK*, **36**, 797 (1998b).

Namkung, W. and Kim, S. D., "Gas Backmixing in the Dense Region of a Circulating Fluidized Bed," *Korean J. Chem. Eng*., **16**, 456 (1999).

Namkung, W., Kim, S. W. and Kim, S. D., "Transition Velocity to Turbulent Fluidized Bed and Flow Regime," *HWAHAK KONGHAK*, **38**, 523 (2000).

Senior, R. C. and Avidan, A. A., "Comparison of the Performance of Circulating and Turbulent Bed FCC Regenerators," Proc. of 5th Int. Conf. on Circulating Fluidized Bed, Beijing, China (1996).

Wilson, J. W., "Fluid Catalytic Cracking–Technology and Operation," Penn Well Publishing Company, Oklahoma, USA (1997).